Probing the serpin structural-transition mechanism in ovalbumin mutant R339T by proteolytic-cleavage kinetics of the reactive-centre loop

Yasuhiro ARII[1] and Masaaki HIROSE[2]

Division of Applied Life Sciences, The Graduate School of Agriculture, Kyoto University, Uji, Kyoto 611-0011, Japan

A mutant ovalbumin (R339T), but not the wild-type protein, is transformed into the canonical loop-inserted, thermostabilized form after the P1–P1′ cleavage [Yamasaki, Arii, Mikami and Hirose (2002) J. Mol. Biol. **315**, 113–120]. The loop-insertion mechanism in the ovalbumin mutant was investigated by proteolytic-cleavage kinetics. The nature of the inserted loop prevented futher cleavage of the P1–P1′ pre-cleaved R339T mutant by subtilisin, which cleaved the second P8–P7 loop site in the P1–P1′ pre-cleaved wild-type protein. After subtilisin proteolysis of the intact R339T, however, two final products that corresponded to the single P1–P1′ and double P1–P1′/P8–P7 cleavages were generated with variable ratios depending on the proteolysis conditions. This was accounted for by the occurrence of two mutually competitive reactions: the loop-insertion reaction and the proteolytic cleavage of the second P8–P7 site in the immediate intermediate after the P1–P1′ cleavage. The competitive nature of the two reactions enabled us to establish a kinetic method to determine the rate constants of the reactions. The first-order rate constant for the loop insertion was determined to be 4.0×10^{-3}/s in the R339T mutant. The second-order rate constant for the P8–P7 cleavage in the immediate P1–P1′ cleavage product for the R339T mutant was > 10 times compared with that for its wild-type counterpart. This highly accessible loop nature may play a crucial role in the loop-insertion mechanism for R339T mutant ovalbumin.

Key words: kinetic serpin mechanism, loop insertion, non-inhibitory serpin.

INTRODUCTION

The serpins are a family of serine proteinase inhibitors, including α_1-proteinase inhibitor [1], antithrombin [2] and plasminogen-activator inhibitor-1 [3]. They share the same three-dimensional structure consisting of three β-sheets and nine α-helices [4]. Their physiological importance and function-related unique structural movement make them one of the major targets of modern bioscience research [5].

The serpins also include a group of non-inhibitory proteins, which have a sequence similar to the inhibitory serpins [5–7]. Previous studies of the serpin mechanism were carried out, often by the 'negative'-mutation approach for inhibitory serpins, where the functional role of an amino-acid residue was evaluated on the basis of the loss of activity in a natural [8] or recombinant mutant [9–11]. Nevertheless, an alternative approach, to give the activity to a non-inhibitory serpin, would provide more direct evidence for the structure–function relationship of serpins. Ovalbumin, a typical non-inhibitory serpin, appears to be the best model for such a 'positive' mutation approach, since it is cleaved at the canonical P1–P1′ site by a serine proteinase [12]. In addition, ovalbumin is the only protein of the non-inhibitory serpins that has been proved to share the common three-dimensional structure of the inhibitory serpins by crystallographic analysis [13–15].

In the inhibitory serpins, the reactive-centre loop is inserted into the central β-sheet after the cleavage at the reactive P1–P1′ site [5,16,17]; this dynamic conformational change that accompanies a marked thermostabilization is suspected to be the crucial step for the exertion of the inhibitory activity [16–19]. Unlike the inhibitory serpins, ovalbumin does not have the ability to undergo the conformational transition into the loop-inserted thermostabilized form after the cleavage at the serpin-specific P1–P1′ site [13,19]. This was considered to be the major reason for a lack of inhibitory activity in egg-white protein. However, we have demonstrated [20] very recently that the defect of the loop-insertion mechanism in ovalbumin can be overcome by a single-hinge mutation at the P14 serpin site that includes the replacement of a bulky Arg^{339} residue by a less-bulky Thr residue, generating the mutant R339T. This has been proven unequivocally by crystallographic and thermodynamic evidence that the ovalbumin mutant R339T is transformed after the P1–P1′ cleavage into the canonical loop-inserted, thermostabilized form [20].

Despite the acquisition of the loop-insertion mechanism, the mutant ovalbumin R339T is still non-inhibitory, at least against elastase and subtilisin (Y. Arii and M. Hirose, unpublished work). In the inhibitory serpins, the insertion of the reactive-centre loop into the central β-sheet after the cleavage at the reactive P1–P1′ site may be a driving force for translocation of the proteinase, trapped at the P1 site, from one side of the serpin to the other side [5,16,17]. The relatively stable nature of the loop-inserted conformer against deacylation is considered to be the molecular basis for the inhibitory activity. The deceleration of the loop-insertion process in inhibitory serpin mutants results in the escape of trapped proteinase [16,17]. Therefore an accelerated loop insertion may be a crucial requisite for the exertion of the inhibitory activity of serpins. This raises the possibility that the non-inhibitory nature of the ovalbumin mutant is related to a decelerated loop-insertion rate. To examine this possibility, direct determination of the loop-insertion rate is essential. Unfortunately no simple and universal method is available.

In the present study, we have established a method to determine directly the loop-insertion rate by simple proteinase-cleavage kinetics. This method utilizes the serpin-loop nature of ovalbumin: the reactive-centre loop is inaccessible to subtilisin in the

[1] Present address: Department of Medicinal Chemistry, Center for Frontier Research in Medicinal Science, Kyoto Pharmaceutical University, Yamashina-ku, Kyoto 607 8412, Japan.

[2] To whom correspondence should be addressed (e-mail hirose@soya.food.kyoto-u.ac.jp).

P1–P1′-cleaved, loop-inserted form but receives the proteolytic cleavage at the P8–P7 site in the pre-loop-inserted intermediate after the P1–P1′ cleavage. We report here that the first-order rate constant for loop insertion after the P1–P1′ cleavage is quite low with a value of 4.0×10^{-3}/s. The kinetic analyses also reveal that the P8–P7 site of R339T immediately after the P1–P1′ cleavage is better accessible by one order of magnitude against the proteinase compared with that of its wild-type counterpart. This strongly suggests that increased accessibility of the R339T loop plays a crucial, or at least partial, role in the subsequent conformational transition of the mutant ovalbumin.

EXPERIMENTAL

Materials

Egg-white ovalbumin was purified by crystallization as described previously [21]. The recombinant wild-type and mutant ovalbumin R339T were prepared as described elsewhere [20,22]. Restriction enzymes and T4 polynucleotide kinase were obtained from TaKaRa Shuzo (Tokyo, Japan). Primer oligonucleotides for the mutation were synthesized by Amersham Pharmacia Biotech (Tokyo, Japan). The protein concentration was estimated from the absorption at 280 nm by using $A^{1\%}_{1\,cm} = 7.12$ [23]. Subtilisin Carlsberg of *Bacillus licheniformis* (protease type VIII), porcine pancreatic elastase (EC 3.4.21.11), trypsin (type XI) and *N*-succinyl-Ala-Ala-Pro-Phe-*p*-nitroanilide were purchased from Sigma (St Louis, MO, U.S.A.). PMSF was obtained from Nacali Tesque (Kyoto, Japan) and other chemicals were from Wako Pure Chemical Industries (Osaka, Japan).

Proteolysis of ovalbumin and SDS/PAGE

The wild-type and R339T mutant proteins were incubated at 0.2 mg/ml and 25 °C in 20 mM sodium phosphate buffer, pH 7.0, with porcine pancreatic elastase or with subtilisin Carlsberg for the indicated time periods. The reaction was terminated by adding 0.1 vol. of 5 % trifluoroacetic acid to the reaction mixture. The samples were mixed with 0.36 vol. of an SDS sample buffer (0.25 M Tris/HCl, pH 7.0, 4 % SDS, 40 % glycerol and 80 mM 2-mercaptoethanol), neutralized by adding 0.06 vol. of 1.0 M Tris base, pretreated in a boiling-water bath for 2 min, and then electrophoresed on a 10 % polyacrylamide gel at a constant current of 12.5 mA for 2.5 h by the standard method of Laemmli [24]. Proteins were stained with 0.25 % Coomassie Brilliant Blue R-250.

Preparation of P1–P1′ pre-cleaved ovalbumin

Recombinant ovalbumin was incubated at 1 mg/ml with 10 μg/ml of porcine pancreatic elastase in 20 mM sodium phosphate buffer, pH 7.0, at 25 °C for 4 h. The proteolysis was terminated by adding 0.015 vol. of 0.1 M PMSF and the mixtures were diluted with 3 vol. of 5 mM sodium phosphate buffer, pH 6.0. The P1–P1′-cleaved protein was purified by using an anion-exchange column (Mono Q 5/5; Amersham Pharmacia Biotech, Tokyo, Japan) as described previously [22].

Quantitative analyses of proteolysis by subtilisin

The P1–P1′ pre-cleaved wild-type and R339T-mutant proteins were incubated at 0.2 mg/ml with 20 ng/ml of subtilisin Carlsberg in 20 mM sodium phosphate, pH 7.0, at 25 °C. At various incubation times, the reaction was terminated by the addition of trifluoroacetic acid and the samples were analysed by SDS/PAGE in the same way. The proteins, visualized by staining with Coomassie Brilliant Blue R-250, were quantified with the software NIH image (version 1.60). For kinetic analysis of the proteolysis of the intact ovalbumin, the wild-type and R339T-mutant proteins were incubated at 0.2 mg/ml (4.4 μM) with various concentrations (5–20 ng/ml: 0.18–0.73 nM) of subtilisin Carlsberg or at various concentrations (4.4–11.1 μM) with 20 ng/ml of the proteinase [25] in 20 mM sodium phosphate buffer, pH 7.0, at 25 °C. The reaction was terminated at different incubation times, and SDS/PAGE and quantification of the protein bands were done in the same way. The rate constants for the proteolysis were estimated by fitting eqns (2)–(8) (see the Results section) to the data by using the KaleidaGraph software (Synergy Software, PA, U.S.A). The subtilisin activity utilized in the present study was 0.27 unit/mg of the proteinase, where 1 unit is defined as the enzyme activity that converts 1 μmol of substrate per minute. The conditions for assaying the enzyme were as follows. At 25 °C, 0.25 mM *N*-succinyl-Ala-Ala-Pro-Phe-*p*-nitroanilide substrate [26] was incubated with various concentrations of subtilisin Carlsberg (0.5–2.0 nM) in 20 mM sodium phosphate buffer, pH 7.0, containing 1 % dimethyl formamide in final volume of 2 ml. The absorbance of the *p*-nitroanilide released was monitored at 410 nm with a Shimazu UV-3000 spectrophotometer (Kyoto, Japan).

RESULTS

Proteolytic patterns of recombinant ovalbumin

Both egg-white and recombinant ovalbumin have been shown to be cleaved by porcine pancreatic elastase at the P1–P1′ site only [12,27]. Using subtilisin Carlsberg, the proteolytic cleavage occurs first at the P1–P1′ site and then at the P8–P7 site [28]. To investigate the cleavage pattern, the wild-type and R339T-mutant proteins were incubated with elastase and/or subtilisin Carlsberg, and then the proteolytic patterns were analysed by SDS/PAGE. As shown in Figure 1, the proteolysis of the wild-type and mutant proteins by elastase yielded the same 39 kDa fragment that can be accounted for by the P1–P1′ cleavage (Figure 1, lanes 2 and 7). P1–P1′ cleavage was confirmed by N-terminal sequence analysis: for either the wild-type or mutant protein, the newly generated N-terminal sequence by elastase proteolysis was Ser-

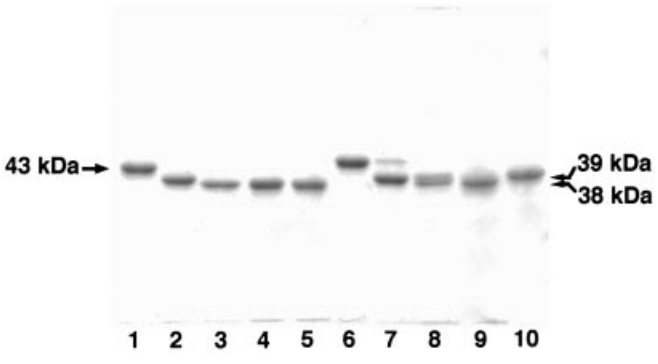

Figure 1 Limited proteolysis of ovalbumin

The wild-type (lanes 1–5) and R339T mutant (lanes 6–10) proteins were incubated at 0.2 mg/ml and 25 °C in 20 mM sodium phosphate buffer, pH 7.0, with 0.2 μg/ml of porcine pancreatic elastase for 20 h (lanes 2 and 7), with 5 ng/ml of subtilisin Carlsberg for 20 h (lanes 3 and 8) or with 200 ng/ml of this proteinase for 1 h (lanes 4 and 9). For lanes 5 and 10, the proteins were incubated first with 0.2 μg/ml of porcine pancreatic elastase for 20 h and then with 200 ng/ml of subtilisin Carlsberg for 1 h (lanes 4 and 9) under the same conditions. Lanes 1 and 6 are controls without proteolysis. The proteins were electrophoresed by SDS/PAGE and stained with Coomassie Brilliant Blue R-250 as described in the text.

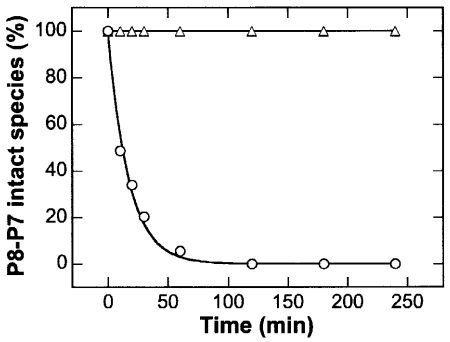

Figure 2 Subtilisin proteolysis of the P1–P1′ pre-cleaved proteins

The P1–P1′ pre-cleaved wild-type (○) and R339T mutant (△) proteins were incubated in duplicate at 0.2 mg/ml and 25 °C with 20 ng/ml (0.73 nM) of subtilisin Carlsberg in 20 mM sodium phosphate buffer, pH 7.0, for various times. The proteins were analysed by SDS/PAGE and the remaining amount of the P1–P1′ pre-cleaved proteins was determined as described in the text. For the P1–P1′ pre-cleaved wild-type protein, curve fitting was performed by a simple first-order reaction; the apparent first-order rate constant was 9.5×10^{-4}/s.

Val-Ser-Glu-Glu-Phe, which corresponded to the sequence from the P1′ residue of Ser[353] to Phe[358] of ovalbumin. The proteolysis of the wild-type protein by subtilisin yielded, at either high or low proteinase concentration, a single 38 kDa fragment corresponding to the second P8–P7 cleavage product (Figure 1, lanes 3 and 4). By subtilisin proteolysis of the mutant protein at high and low enzyme concentrations, respectively, a single fragment by the second P8–P7 cleavage and two fragments by the first P1–P1′ and the second P8–P7 cleavages were produced (Figure 1, lanes 8 and 9). When proteolysis was done first by elastase and then by high concentration of subtilisin, however, the P1–P1′-cleaved mutant protein was not further cleaved at the P8–P7 site, whereas the wild-type protein underwent proteolysis at the second P8–P7 cleavage site (Figure 1, lanes 5 and 10).

To confirm the differential P8–P7 accessibility after the P1–P1′ cleavage, we prepared the P1–P1′ pre-cleaved wild-type and mutant ovalbumins in purified forms by protein incubation with elastase and subsequent anion-exchange chromatography, and then analysed for their accessibilities to subtilisin cleavage. Figure 2 clearly displays that the P1–P1′ pre-cleaved mutant was not further cleaved by subtilisin, whereas the second cleavage occurs in the P1–P1′ pre-cleaved wild-type protein under the same proteolysis condition. These results indicate that, after the cleavage at the P1–P1′ site, the P8–P7 site of the R339T mutant is transformed, according to the structural transition by the loop insertion [20], into an inaccessible loop state against subtilisin attack.

Time course for subtilisin proteolysis of the intact proteins

The above results suggest that the intact form, but not the P1–P1′ pre-cleaved form, of the mutant protein receives the second P8–P7 cleavage by subtilisin (Figures 1 and 2). To investigate the differential second-cleavage mechanism, we examined the time course of subtilisin proteolysis with the intact protein substrates. As shown in Figure 3, the P1–P1′-cleaved product from the wild-type protein tentatively increased initially, but then decreased with the progress of proteolysis at both subtilisin concentrations of 10 and 20 ng/ml (Figures 3A and 3C). With the R339T mutant, however, the P1–P1′-cleaved product increased and then reached a plateau at both concentrations of proteinase (Figures 3B and 3D). Another important observation for the mutant

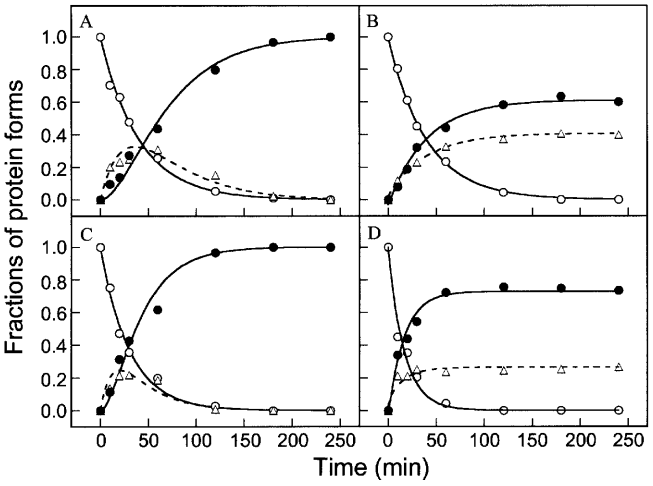

Figure 3 Time courses for the loop cleavages by subtilisin

The wild-type (**A**, **C**) and R339T mutant (**B**, **D**) proteins were incubated in duplicate at 4.4 μM and 25 °C in 20 mM sodium phosphate buffer, pH 7.0, with 0.37 nM (**A**, **B**) or 0.73 nM (**C**, **D**) of subtilisin Carlsberg. At different incubation times, the proteolysis was terminated and the fractions of the intact protein (○), P1–P1′-cleaved form (△) and P1–P1′/P8–P7-cleaved form (●) were analysed by SDS/PAGE as described in the text. Curve fittings were carried out by using eqns (3)–(7) as described in the text.

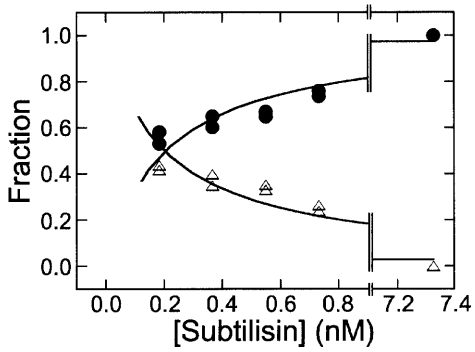

Figure 4 Plateau levels of the P1–P1′-cleaved and P1–P1′/P8–P7-cleaved forms during the subtilisin proteolysis of the R339T mutant

The R339T-mutant protein was incubated in duplicate with various concentrations of subtilisin Carlsberg and the time courses of the proteolysis were analysed in the same way as described in the legend of Figure 3. The plateau levels of the P1–P1′-cleaved (△) and P1–P1′/P8–P7-cleaved (●) forms that were obtained from the values at 240 min incubation were plotted as a function of subtilisin concentrations. The ordinate represents the fraction of each plateau level. Curve-fitting analyses were carried out on the basis of two mutually competitive reactions in the P1–P1′-cleaved R339T mutant: one is the conformational transition into the subtilisin-resistant thermostabilized form and the other is the P8–P7 cleavage reaction. The rate for the former reaction should be independent of proteinase concentrations, whereas that for the latter reaction depends linearly on proteinase concentration. The fraction for the loop-inserted P1–P1′-cleaved form ($\alpha 1$) and that for the P1–P1′/P8–P7-cleaved form ($\alpha 2$) can therefore be shown as follows: $\alpha 1 = \beta/(\beta + [\text{subtilisin}])$ and $\alpha 2 = [\text{subtilisin}]/(\beta + [\text{subtilisin}])$, where β is a constant in the unit of concentration. The β-value obtained by the curve-fitting analysis was 0.20 nM.

protein was that the plateau level of the P1–P1′-cleaved product decreased with the increase in the subtilisin concentration (Figures 3B and 3D). This relationship is displayed more clearly in Figure 4. The same time-course analyses were carried out at a variety of subtilisin concentrations, and plateau levels of the P1–P1′- and P8–P7-cleaved forms were plotted as a function of the subtilisin concentrations. The plateau level of the P1–P1′-cleaved

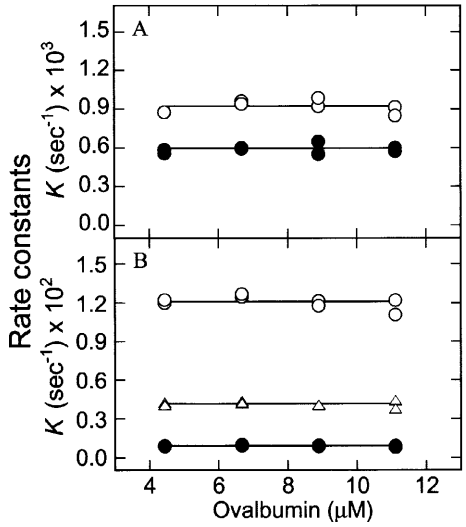

Figure 5 Observed rate constants for the loop insertion and cleavages at various ovalbumin concentrations

The wild-type (**A**) and R339T mutant (**B**) proteins were incubated at various concentrations with 0.73 nM of subtilisin Carlsberg and the time courses of the proteolytic cleavages were obtained in the same way as described in the legend of Figure 3. The rate constants obtained by the same curve-fitting analysis were plotted as a function of the ovalbumin concentrations. The observed rate constants are shown by ●, ○ and △ for K_1, K_2 and K_3, respectively.

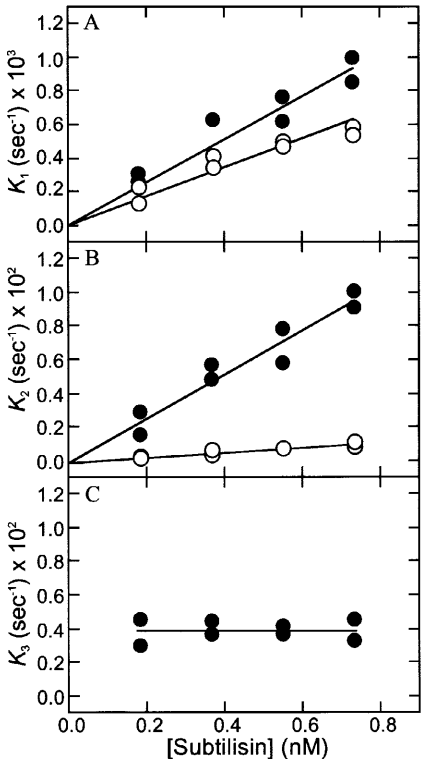

Figure 6 Effect of subtilisin concentrations on the observed rate constants

The wild-type (○) and R339T mutant (●) proteins were incubated at 0.2 mg/ml (4.4 μM) with various concentrations of subtilisin Carlsberg and the time courses of the proteolytic cleavages were obtained in the same way as described in the legend of Figure 3. The apparent rate constants for K_1 (**A**), K_2 (**B**) and K_3 (**C**) obtained by the same curve-fitting analysis were plotted as functions of the subtilisin concentrations.

form decreased with increase in subtilisin concentrations, whereas that of the P8–P7-cleaved form increased. The results from curve-fitting analysis of the data (Figure 4) were consistent with the occurrence of two mutually competitive reactions in the P1–P1′-cleaved R339T mutant: one is the conformational transition into the subtilisin-resistant, loop-inserted form and the other is the P8–P7 cleavage reaction.

Kinetic analysis for the proteolytic cleavage by subtilisin

The Michaelis constant (K_m) for a proteinase is known to be relatively high for the protein substrate. When the concentration of a substrate is significantly lower than the K_m value, as in the present study (see Figure 5), the enzyme reaction is equivalent to a first-order reaction with a rate constant K that can be related to K_m by the equation $K = j[E]/K_m$, where [E] is the enzyme concentration and j the first-order rate constant for the product formed from the ES complex. When the constant K is expressed as the product ($K = k[E]$) of a second-order rate constant k (since $k = j/K_m$) and the enzyme concentration [E], K corresponds to a pseudo-first-order rate constant.

The cleavage pathway of the mutant protein by subtilisin proteolysis is shown by the inclusion of the two competitive reactions in the P1–P1′-cleaved form as follows:

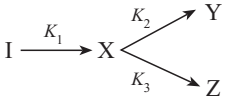

Scheme 1

In Scheme 1, **I** and **X** are the intact form and the P1–P1′-cleaved, non-loop-inserted form, respectively. **Y** is the P1–P1′/P8–P7-cleaved form and **Z** is the P1–P1′-cleaved, loop-inserted form. K_1 and K_2 are the pseudo-first-order rate constants for the proteolysis reactions by subtilisin related to the corresponding second-order rate constants k_1 and k_2, respectively:

$$K_1 = k_1[E] \quad (1)$$

$$K_2 = k_2[E] \quad (2)$$

The constant K_3 should be a true first-order rate constant, since it is the rate constant for the structural transition. $I(t)$ and $Y(t)$, which are defined as the fractions of **I** and **Y**, respectively, at a proteolysis time t, can be expressed as follows:

$$I(t) = \exp(-K_1 t) \quad (3)$$

$$Y(t) = \frac{K_2}{K_2+K_3} - \frac{K_2}{K_2+K_3-K_1}\exp(-K_1 t) + \frac{K_1 K_2}{(K_2+K_3)(K_2+K_3-K_1)}\exp[-(K_2+K_3)t] \quad (4)$$

Defining $X(t)$ and $Z(t)$ as the fractions of **X** and **Z** respectively at a proteolysis time t, the total P1–P1′-cleaved fragment $X(t)+Z(t)$, which can be detected as a band in the gel electrophoresis analysis, is expressed as follows:

$$X(t)+Z(t) = \frac{K_3}{K_2+K_3} + \frac{K_1-K_3}{K_2+K_3-K_1}\exp(-K_1 t) - \frac{K_1 K_2}{(K_2+K_3)(K_2+K_3-K_1)}\exp[-(K_2+K_3)t] \quad (5)$$

Table 1 Rate constants for loop insertion and cleavage

As defined in the text, k_1 and k_2 are the second-order rate constants for the cleavages of P1–P1′ and P8–P7 sites, respectively. K_3 is the first-order rate constant for the loop-insertion reaction.

	Rate constants			
	k_1* ($M^{-1} \cdot s^{-1} \times 10^{-5}$)	k_2* ($M^{-1} \cdot s^{-1} \times 10^{-5}$)	k_2† ($M^{-1} \cdot s^{-1} \times 10^{-5}$)	K_3* ($s^{-1} \times 10^3$)
Wild-type	7.9	13.4	13.0	–
R339T	12.4	140.0	–	4.0

* Data from Figure 6.

† Estimated from the pseudo-first-order rate constant for the P8–P7 cleavage reaction in the P1–P1′ pre-cleaved wild-type protein (Figure 2): the pseudo-first-order rate constant 9.5×10^{-4}/s was divided by the subtilisin concentration 0.73 nM.

For the wild-type protein, no loop-insertion reaction is included ($k_3 = 0$; $\mathbf{Z} = 0$). Eqns (4) and (5) are therefore simplified as follows:

$$Y(t) = 1 - \frac{K_2}{K_2 - K_1}\exp(-K_1 t) + \frac{K_1}{K_2 - K_1}\exp(-K_2 t) \quad (6)$$

$$X(t) = \frac{K_1}{K_2 - K_1}[\exp(-K_1 t) - \exp(-K_2 t)] \quad (7)$$

By using eqns (3)–(7), curve-fitting analyses of the time-course data were carried out at various combinations of subtilisin and ovalbumin concentrations and the first-order rate constants were obtained. The curve-fitting analysis worked well, as demonstrated in Figure 3 in some instances. When the first-order rate constants obtained at a subtilisin concentration of 0.73 nM were plotted as a function of ovalbumin concentrations (4.4–11.1 μM), all the constants showed fixed values, as shown in Figure 5. The observation was reasonable for Scheme 1 in which the rate constants K_1, K_2 and K_3 include no ovalbumin concentration term [for K_1 and K_2, see eqns (1) and (2)], and hence confirms the first-order reaction for the subtilisin proteolysis at the ovalbumin concentrations employed. Eqns (1) and (2) represent K_1 and K_2 as pseudo-first-order rate constants that depend on the proteinase concentrations. This was indeed the case as demonstrated in Figures 6(A) and 6(B): the K_1 and K_2 values linearly depended on the subtilisin concentrations for either the wild-type or mutant protein, whereas a true first-order rate constant K_3 shows an invariable value at varying subtilisin concentrations. According to eqns (1) and (2), the second-order rate constants k_1 and k_2 can be obtained from the slopes of the K_1 and K_2 plots. Table 1 summarizes the values for the second-order rate constants k_1 and k_2 and the first-order rate constant K_3. One of the most important observations was that the rate constant for the loop-insertion K_3 was directly determined to be 4.0×10^{-3}/s for the R339T mutant. Although the absolute values of k_1 and k_2 may be variable depending on the specific activity of the proteinase, their relative ratios for the wild-type and mutant proteins should provide useful information. A surprising observation was that the k_2 value for the mutant protein was one order of magnitude greater than that for the wild-type protein, whereas the k_1 value for the former protein was greater by only approx. 1.5-fold compared with the latter protein. The second-order rate constant k_2 for the wild-type protein was almost the same as the values obtained from the subtilisin-cleavage reactions of the intact and P1–P1′ pre-cleaved proteins (Table 1).

DISCUSSION

In the inhibitory serpins, the reactive-centre loop is inserted into the central β-sheet after the cleavage at the reactive P1–P1′ site [5,16,17]. This dynamic conformational transition accompanies a marked increase in the protein thermostability and is believed to be a crucial process for the inhibitory function [16–19]. In ovalbumin, a non-inhibitory member of the serpin superfamily [5–7], the canonical cleavage is at the P1–P1′ site by a serine proteinase but does not undergo the structural transition into a thermostabilized form after the cleavage [13,19]. The absence of the conformational transition has been hypothesized to be due to the presence of a bulky residue of Arg^{339} at the P14 site in ovalbumin, which functions as a hinge residue in inhibitory serpins on the movement of the reactive-centre loop [5,9]. In a previous study, we have demonstrated by crystallographic and thermodynamic evidence that this is indeed the case; an ovalbumin mutant R339T, with replacement of the P14 hinge residue, undergoes a marked thermostabilization ($\Delta T_m = 15.8$ °C) and the canonical serpin structural transition into the fully loop-inserted form after the P1–P1′ cleavage [20]. An alternative ovalbumin mutant R339S has been shown to be thermostabilized with a reduced ΔT_m value of 11 °C after the P1–P1′ cleavage [27]; the P1–P1′ pre-cleaved R339S displays some accessibility to subtilisin on the P8–P7 site. On the basis of these properties, the P1–P1′-cleaved R339S has been hypothesized to be a partially loop-inserted product in which the P15–P10 residues, but not the P9–P1 residues, are inserted [27]. According to the full-loop insertion structure of cleaved R339T [20], Thr^{339}-CG2 undergoes van der Waals interactions with side-chain atoms of Trp^{184} (CZ2 and CH2) and of Phe^{234} (CE1 and CZ), thereby probably working as stabilization factors for the loop-inserted conformation. These van der Waals interactions should be abolished in cleaved R339S. The Thr-residue-related van der Waals interactions may play a crucial role in the correct loop-insertion mechanism in ovalbumin.

The ovalbumin mutant R339T, despite its ability to undergo a transition into a thermostabilized form after the P1–P1′ cleavage, does not show any inhibitory activity against serine proteinases, including elastase and subtilisin Carlsberg (Y. Arii and M. Hirose, unpublished work). In the inhibitory serpins, the reactive-centre loop insertion into the central β-sheet is considered to be a driving force for translocation of the proteinase, trapped at the P1 site, from one side of the serpin to the distal side [5,16,17]. Decreased deacylation rate in the loop-inserted conformer is considered to be the molecular basis for the inhibitory activity. The extent of serpin inhibition should therefore depend on the relative ratio of the rates for the loop insertion and deacylation. This stresses the importance of an accelerated rate of loop insertion for the serpin inhibitory activity.

The inaccessible nature of the P1–P1′ pre-cleaved R339T mutant against subtilisin (Figure 2) led us to establish a quantitative method to analyse the thermostabilization mechanism by proteolytic-cleavage kinetics of the serpin loop. The kinetic model included two mutually competitive first-order reactions in an immediate product after the P1–P1′ cleavage: one is the conformational transition into the subtilisin-resistant, thermostabilized form and the other is the P8–P7 cleavage reaction (Scheme 1). On the basis of the model, the quantitative equations [eqns (3)–(7)] were newly introduced and the kinetic constants were obtained by curve-fitting analysis of the proteolysis data. The curve-fitting analysis was also employed to justify the model that included the first-order reactions for all the kinetic steps (Figure 6). One of the most important results was that the first-order rate constant for the conformational transition was

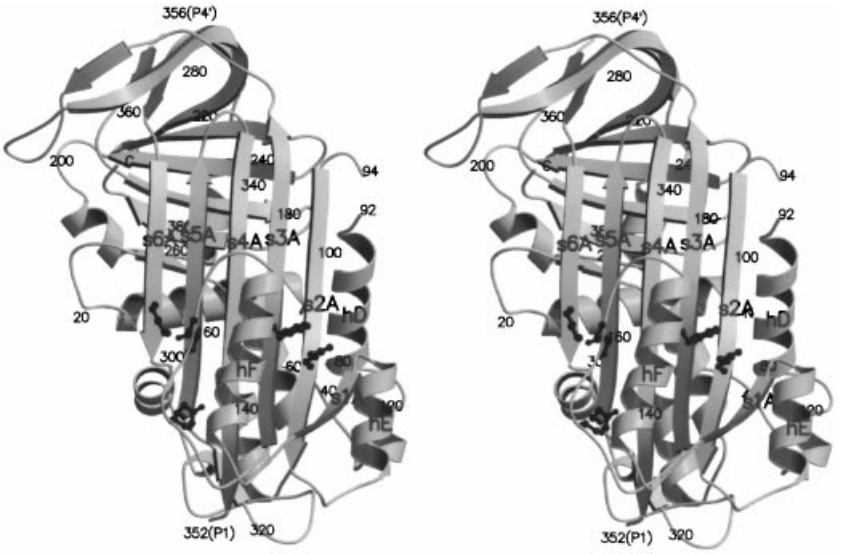

Figure 7 Stereo diagram of the P1–P1′-cleaved structure of ovalbumin mutant R339T

The Figure was produced with MOLSCRIPT [36] and Raster 3D [37] by using the PDB data (code no. 1JTI) for P1–P1′-cleaved ovalbumin mutant R339T [20]. Strands 1A, 2A, 3A, 4A, 5A and 6A that constitute sheet A are labelled s1A, s2A, s3A, s4A, s5A and s6A, respectively. The labelled hD, hE and hF represent helices D, E and F, respectively. The atoms of the amino-acid residues that participate in the interactions of helix F and its descending loop with sheet A (see text) are shown by small filled circles.

clearly determined to be 4.0×10^{-3}/s for the R339T mutant. In previous reports, the first-order rate constant for the loop insertion in an inhibitory serpin, plasminogen activator inhibitor-1 has been estimated by fluorescence resonance-energy-transfer measurements to be 3.4/s [29] or a value more than one order of magnitude of this [30]. The first-order rate constant for the loop insertion in the present R339T mutant (4.0×10^{-3}/s) is lower by at least three orders of magnitude than that of the inhibitory serpin. Therefore the absence of inhibitory activity in the R339T mutant may be accounted for, at least partially, by a lower rate of loop insertion compared with the deacylation rate.

The decelerated loop-insertion rate in the R339T mutant may be accounted for by restricted motion, relative to sheet A, of helices E and F and of the loop-descending helix F; the conformational situations of the secondary-structure elements in the P1–P1′-cleaved, loop-inserted form are displayed in Figure 7. According to the structural-motion analysis for an inhibitory serpin, α_1-antitrypsin [20], the large contiguous segment that comprises the secondary-structure elements of strands 1A, 2A and 3A, and helices E and F move significantly upon loop insertion, thereby probably leaving room for the reactive-centre loop to be inserted as strand 4A. In the ovalbumin mutant, however, little motion is detected in the entire segments of helix E and the loop-descending helix F, and the motion of helix F itself is also significantly restrained [20]; the restrained motion of these segments may force upon the loop insertion a perturbed sliding of strands 1A, 2A and 3A [20]. The absence of any significant motion of helix E is probably due to the unique occurrence of a disulphide bond (Cys^{73}–Cys^{120}), which links helix E and the loop preceding helix D. The restrained motion in helix F and in its descending loop may be related to the multiple interactions of these segments with sheet A, which are mostly absent in the inhibitory serpins. As a first interaction, two main-chain oxygen atoms Asn^{159}–O and Val^{160}–O in the extended loop-descending helix F receive hydrogen bonds from Lys^{290}–NZ on strand 6A (Figure 7). Secondly, Ser^{165}–O in the same extended loop makes hydrogen bonds with Gln^{325}–NE2 on strand 5A. Thirdly, the indole-ring plane of Trp^{148} of helix F and the plane formed by the NH1, NH2, CZ and NE atoms of Arg^{104} on strand 2A appear to make the stacking-like interaction.

These increased interactions may also contribute to a higher inherent stability of intact ovalbumin than inhibitory serpins [25,31,32]. The importance of destabilized native interactions between helix F and sheet A has been pointed out for the inhibitory activity of α_1-antitrypsin [33]; filling a cavity around Gly^{117} of strand 2A by a bulkier residue, which confers an increased stability on the inhibitor, resulted in decelerated loop insertion and in decreased inhibitory activity. Likewise, C1 inhibitor shows a less efficient inhibitory activity at 4 °C than at 38 °C [34], which indicates the importance of less-stabilized conformational flexibility for serpin inhibitory activity. These may imply that a high-temperature condition is favoured for possible detection of the inhibitory activity of ovalbumin mutants.

An alternative important observation obtained in the present study was that the second-order rate constant for the P8–P7 cleavage is greater by one order of magnitude for the R339T mutant than for its wild-type counterpart (Table 1). Subtilisin Carlsberg cleaves ovalbumin first at the P1–P1′ site and then at the P8–P7 site [28]. According to the crystal structure of intact ovalbumin [14,15], the P1–P1′ and P8–P7 sites are both located in the α-helical part of the loop. The former site appears to be exposed to the environment, whereas the latter site is buried in an interface between the loop and the main core body of the protein. The structural situations of the two sites are consistent with the occurrence of the primary cleavage at the P1–P1′ site. Subsequent loop insertion requires a large-scale motion and conformational transition for most part of the reactive-centre loop [14,20]. The extent of the loop motion, leaving from the main protein body, should be much greater in the P1–P1′-cleaved R339T than in the wild-type. The accelerated rate of the second cleavage in R339T may reflect this structural situation of the loop that makes the P8–P7 site more accessible. Alternatively, the reactive-centre loop of R339T may assume an unfolded conformation during

the structural transition from α-helix to the loop-inserted β-strand (strand 4A). The presence of such an unfolded state may be related to the accelerated cleavage of the R339T loop. Irrespective of the detailed mechanisms, the accelerated-loop cleavage in P1–P1′-cleaved R339T may reflect the unique structural feature of a pre-loop-inserted intermediate crucial for the subsequent loop insertion.

In conclusion, a simple method for determining the rate of the loop insertion was established for an ovalbumin mutant by this study. The 'positive'-mutation approach to give the inhibitory activity to ovalbumin should provide direct evidence for the structure–function relationship of serpins. In a previous study utilizing fusion proteins of ovalbumin and plasminogen-activator inhibitor-2, the acquisition of the inhibitory activity was attained by a large-scale structural rearrangement that included 64% replacement of ovalbumin peptide sequence by the corresponding sequence of the inhibitory serpin [35]. The acquisition of an accelerated loop-insertion rate is considered to give the inhibitory activity to ovalbumin by a minimum replacement of amino-acid residues. The present method should provide a crucial probe for monitoring the structural and functional studies of logically designed ovalbumin on the basis of the crystal structure [20].

This work was supported in part by a grant-in-aid for scientific research from the Ministry of Education, Science, Sports and Culture of Japan. We are grateful to Dr Masayuki Yamasaki for his help in simulating the three-dimensional structure of serpin.

REFERENCES

1 Löebermann, H., Tokuoka, R., Deisenhofer, J. and Huber, R. (1984) Human α_1-proteinase inhibitor. Crystal structure analysis of two crystal modifications, molecular model and preliminary analysis of the implications for function. J. Mol. Biol. **177**, 531–557

2 Carrell, R. W., Stein, P. E., Fermi, G. and Wardell, M. R. (1994) Biological implications of a 3 Å structure of dimeric antithrombin. Structure **2**, 257–270

3 Mottonen, J., Strand, A., Symersky, J., Sweet, R. M., Danley, D. E., Geoghegan, K. F., Gerard, R. D. and Goldsmith, E. J. (1992) Structural basis of latency in plasminogen activator inhibitor-1. Nature (London) **355**, 270–273

4 Gettins, P. E. W., Patston, P. A. and Schapira, M. (1993) The role of conformational change in serpin structure and function. BioEssays **15**, 461–467

5 Huber, R. and Carrell, R. W. (1989) Implications of the three-dimensional structure of α_1-antitrypsin for structure and function of serpins. Biochemistry **28**, 8951–8966

6 Patston, P. A. and Gettins, P. G. W. (1996) Significance of secondary structure predictions on the reactive center loop region of serpins: a model for the folding of serpins into a metastable state. FEBS Lett. **383**, 87–92

7 Whisstock, J., Skinner, R. and Lesk, A. M. (1998) An atlas of serpin conformations. Trends Biochem. Sci. **23**, 63–67

8 Stein, P. E. and Carrell, R. W. (1995) What do dysfunctional serpins tell us about molecular mobility and disease? Nat. Struct. Biol. **2**, 96–113

9 Hood, D. B., Huntington, J. A. and Gettins, P. G. W. (1994) α1-Proteinase inhibitor variant T345R. Influence of P14 residue on substrate and inhibitory pathways. Biochemistry **33**, 8538–8547

10 Chaillan-Huntington, C. E., Gettins, P. G. W., Huntington, J. A. and Patston, P. A. (1997) The P6-P2 region of serpins is critical for proteinase inhibition and complex stability. Biochemistry **36**, 9562–9570

11 Davis, III, A. E., Aulak, K., Parad, R. B., Stecklein, H. P., Eldering, E., Hack, C. E., Kramer, J., Strunk, R. C., Bissler, J. and Rosen, F. S. (1992) C1 inhibitor hinge region mutations produce dysfunction by different mechanisms. Nat. Genet. **1**, 354–358

12 Wright, H. T. (1984) Ovalbumin is an elastase substrate. J. Biol. Chem. **259**, 14335–14336

13 Wright, H. T., Qian, H. X. and Huber, R. (1990) Crystal structure of plakalbumin, a proteolytically nicked form of ovalbumin. Its relationship to the structure of cleaved α_1-proteinase inhibitor. J. Mol. Biol. **213**, 513–528

14 Stein, P. E., Leslie, A. G. W., Finch, J. T., Turnell, W. G., McLaughlin, P. J. and Carrell, R. W. (1990) Crystal structure of ovalbumin as a model for the reactive centre of serpins. Nature (London) **347**, 99–102

15 Stein, P. E., Leslie, A. G. W., Flinch, J. T. and Carrell, R. W. (1991) Crystal structure of uncleaved ovalbumin at 1.95 Å resolution. J. Mol. Biol. **221**, 941–959

16 Huntington, J. A., Read, R. J. and Carrell, R. W. (2000) Structure of a serpin-protease complex shows inhibitory by deformation. Nature (London) **407**, 923–926

17 Engh, R. A., Huber, R., Bode, W. and Schulze, A. J. (1995) Divining the serpin inhibition mechanism: a suicide substrate 'springe'? Trend Biotech. **13**, 503–510

18 Wright, H. T. and Scarsdale, J. N. (1995) Structural basis for serpin inhibitor activity. Proteins **22**, 210–225

19 Stein, P. E., Tewkesbury, D. A. and Carrell, R. W. (1989) Ovalbumin and angiotensinogen lack serpin S-R conformational change. Biochem. J. **262**, 103–107

20 Yamasaki, M., Arii, Y., Mikami, B. and Hirose, M. (2002) Loop-inserted and thermostabilized structure of P1-P1′ cleaved ovalbumin mutant R339T. J. Mol. Biol. **315**, 113–120

21 Tatsumi, E., Takahashi, N. and Hirose, M. (1994) Denatured state of ovalbumin in high concentrations of urea as evaluated by disulfide rearrangement analysis. J. Biol. Chem. **269**, 28062–28067

22 Arii, Y., Takahashi, N., Tatsumi, E. and Hirose, M. (1999) Structural properties of recombinant ovalbumin and its transformation into a thermostabilized form by alkaline treatment. Biosci. Biotechnol. Biochem. **63**, 1392–1399

23 Glazer, A. N., McKenzie, H. A. and Wake, R. G. (1963) The denaturation of proteins. II. Ultraviolet absorption spectra of bovine serum albumin and ovalbumin in urea and in acid solution. Biochim. Biophys. Acta **69**, 240–248

24 Laemmli, U. K. (1970) Cleavage of structural proteins during the assembly of the head of bacteriophage T4. Nature (London) **227**, 680–685

25 Takahashi, N., Tatsumi, E., Orita, T. and Hirose, M. (1996) Role of the intrachain disulfide bond of ovalbumin during conversion into S-ovalbumin. Biosci. Biotech. Biochem. **60**, 1464–1468

26 DelMar, E. G., Largman, C., Brodrick, J. W. and Geokas, M. C. (1979) A sensitive new substrate for chymotrypsin. Anal. Biochem. **99**, 316–320

27 Huntington, J. A., Fan, B., Karlsson, K. E., Deinum, J., Lawrence, D. A. and Gettins, P. G. W. (1997) Serpin conformational change in ovalbumin. Enhanced reactive center loop insertion through hinge region mutations. Biochemistry **36**, 5432–5440

28 Ottesen, M. (1958) Transformation of ovalbumin into plakalbumin. A case of limited proteolysis. Compt. Rend. Trav. Lab. Carlsberg **30**, 211–270

29 Shore, J. D., Day, D. E., Francis-Chmura, A. M., Verhamme, I., Kvassaman, J., Lawrence, D. A. and Ginsburg, D. (1995) A fluorescent probe study of plasminogen activator inhibitor-1. Evidence for reactive center loop insertion and its role in the inhibitory mechanism. J. Biol. Chem. **270**, 5395–5398

30 Olson, S. T., Swanson, R., Day, D., Verhamme, I., Kvassman, J. and Shore, J. D. (2001) Resolution of Michaelis complex, acylation, and conformational change steps in the reactions of the serpin, plasminogen activator inhibitor-1, with tissue plasminogen activator and trypsin. Biochemistry **40**, 11742–11756

31 Kaslik, G., Kardos, J., Szabo, E., Szilagyi, L., Zavodszky, P., Westler, W. M., Makley, J. L. and Graf, L. (1997) Effects of serpin binding on the target proteinase: Global stabilization, localized increased structural flexibility, and conserved hydrogen bonding at the active site. Biochemistry **36**, 5455–5464

32 Lee, K. N., Im, H., Kang, S. W. and Yu, M. H. (1998) Characterization of a human α_1-antitrypsin variant that is as stable as ovalbumin. J. Biol. Chem. **273**, 2509–2516

33 Lee, C., Park, S. H., Lee, M. Y. and Yu, M. H. (2000) Regulation of protein function by native metastability. Proc. Natl. Acad. Sci. U.S.A. **97**, 7727–7731

34 Patston, P. A., Gettins, P., Beechem, J. and Schapira, M. (1991) Mechanism of serpin action: evidence that C1 inhibitor functions as a suicide substrate. Biochemistry **30**, 8876–8882

35 McCarthy, B. J. and Worrall, D. M. (1997) Analysis of serpin inhibitory function by mutagenesis of ovalbumin and generation of chimeric ovalbumin/PAI-2 function proteins. J. Mol. Biol. **267**, 561–569

36 Kraulis, P. J. (1991) MOLSCRIPT: a program to produce both detailed and stereochemical quality of protein structures. J. Appl. Cryst. **24**, 946–950

37 Merritt, E. A. and Bacon, D. J. (1997) Raster3D: photorealistic molecule graphics. Methods Enzymol. **277**, 505–524

Received 10 October 2001/21 January 2001; accepted 11 February 2002